J Mater Sci (2008) 43:6866–6871
DOI 10.1007/s10853-008-3016-0

Changes in tensile properties for the PET films by the treatment in supercritical carbon dioxide fluid

Yutaka Kawahara · Tomohiro Kurooka · Dohiko Terada

Received: 30 May 2008 / Accepted: 22 September 2008 / Published online: 11 October 2008

Abstract Poly (ethylene terephthalate) films were treated in supercritical CO_2 (s-CO_2) fluid, and the modifications in tensile properties were investigated. The yield load peaks became ambiguous and the breaking strains and loads decreased for the treated films. However, the tensile modulus and the yield strain were almost unchanged after the treatments. The yield strain is related to the interplay between the amorphous entanglement density and the stability of crystal blocks. WAXD patterns for the films were hardly modified through the treatment. Thus the orientation for the crystal blocks seems to be unchanged. Moreover, laser Raman microprobe spectroscopic analyses revealed that the orientation of molecular chains is almost retained after the treatments. Thus it is natural to assume that the interplay between the amorphous entanglement density and the stability of crystal blocks will also be kept constant even though the swelling of amorphous regions with s-CO_2 occurs during the treatments. From differential scanning calorimetry measurements, it was found that the heat of fusion for the crystallites was a little increased without shifting the peak position after the treatment. Therefore, the increase in crystallinity is not due to the thickening or crystal perfecting for primary lamellae, but due to the secondary crystallization. The increase in crystallinity caused by the secondary lamellae crystallized and combined onto the primary lamellae seems to have reduced the amorphous chains to be deformed easily at tensile tests. Then the breaking strains and loads decreased for the treated films.

Y. Kawahara (✉)
Department of Chemistry and Chemical Biology, Gunma University, 1-5-1 Tenjin-cho, Kiryu, Gunma 376-8515, Japan
e-mail: kawahara@chem-bio.gunma-u.ac.jp; kawahara@bce.gunma-u.ac.jp

T. Kurooka · D. Terada
Division of Advanced Fibro-Science, Graduate School, Kyoto Institute of Technology, Matsugasaki, Sakyo-ku, Kyoto 606-8585, Japan

Introduction

Poly (ethylene terephthalate) (PET) fibers and films have been widely used due to their excellent physical properties. As for the formation of film structure several investigations have been made [1–3]. These results suggest that the slipping and/or the entanglement of adjacent molecular chains during the drawing process influence the formation of film structure as well as the resulting physical properties of the film. In the previous work [4], the stabilizing effects of amorphous chains by the imperfect small crystallites [5] generated in amorphous regions via the treatment in supercritical CO_2 (s-CO_2) fluid were discussed from the changes in the viscoelastic properties. The peak intensity of loss modulus, E'' for s-CO_2-treated PET fibers was obviously weakened and the peak position was shifted to the higher temperature side. Therefore, if such structural modification occurs in the amorphous regions of PET films through the treatment in s-CO_2, the physical properties for the treated films will be affected.

In this article, PET films were subjected to the s-CO_2 treatment, and the changes in tensile properties were investigated.

Experimental parts

PET films

A roll of PET film of 16 μm in thickness supplied from TEIJIN Co. Ltd. (Osaka, Japan) was used. Density of the film was 1.399 g/cm^3 that was measured using a density gradient column prepared from calcium nitrate at 25 °C.

s-CO_2 treatments

s-CO_2 fluid treatment (SFT) was made as follows. The films without fixing the ends were put into a tube and s-CO_2 fluid of 40 °C flowed into the tube. Then, the temperature of the tube was raised up to 100 °C and the pressure was controlled to 25 MPa. The treatment was made for 60 min.

Measurements

A shrinkage ratio, R, was calculated by measuring a length between corresponding points marked on a film. R (%) = 100 × (L_0 − L)/L_0, where L_0 and L are the lengths before and after the SFT, respectively.

The films were cut into a rectangular shape of 40 mm in length and 5 mm in width. The tensile tests were made in a machine direction (MD) and a transverse direction (TD) at 20 °C and 65% RH using an automatic Tensilon Tester (A&D, type STA-1150, Tokyo, Japan). The gauge length was 20 mm and the crosshead speed was 10 mm/min. The values were the averages of 15 tests at least.

The differential scanning calorimetry (DSC) measurement was performed using a DSC-3100 (Brukeraxs Co., Tokyo, Japan) at a heating rate of 10 °C/min in a nitrogen gas atmosphere. The weight of the sample was about 2 mg. Cold crystallization was not observed for the films. From the endothermic area, ΔH_{obs}, in the temperature range in which the melting peak appears, the degree of crystallinity, X_c, was estimated using the equation. X_c (%) = 100 × ($\Delta H_{obs}/\Delta H_f$), where ΔH_f is the heat of fusion of perfectly crystalline PET of 121 J/g [6]. At the calculation of crystallinity, the fusion enthalpy for imperfect crystallites observed in case of s-CO_2-treated films was not included.

X-ray diffraction patterns were recorded using a Laue camera. Ni-filtered and pinhole-collimated CuKα X-rays generated at 40 kV, 18 mA were used. The camera length was 47.5 mm, and the exposure time was 60 min.

Laser Raman microprobe spectroscopy was made using a JRS-SYS 2000KKW (JEOL, Tokyo, Japan) changing the polarization direction of incident laser beam by the rotation of a polarizer. The analyzer slit is always settled parallel to the polarization direction of incident laser beam.

Results and discussion

The aspect for the film was almost retained after the SFT. The shrinkages measured in MD and TD were 0.9 and 0.6%, respectively. In the conventional polymerization process of PET, it is inevitable to synthesize oligomers as impurity fractions. In addition, PET fibers and films tend to be swollen to hydrophobic s-CO_2 fluid, which will promote the oligomer migration. Therefore the oligomer deposition can be observed for PET fibers and films when those are subjected to SFT [4, 7]. Figure 1 shows the surface of the film after SFT. Crystalloid oligomer particles can be observed.

The WAXD patterns for the thru-view and the edge-view for the films are shown in Fig. 2. It is seen that (−112) diffraction in the thru-view for the control films has expanded like a Debye-Scherrer ring (see Fig. 2a). However the broad diffraction intensity peaks of (−112) can still be recognized in the direction of Azimuthal angle of 45° from the meridian. Such WAXD pattern suggests that the films used in this study have been produced via the widely used successive-biaxial stretching method [2, 3]. The diffraction pattern for the edge-view measured for the s-CO_2-treated film has become a little denser. This suggests that crystallinity of the film increased through SFT. However, it is seen that the features for the diffraction patterns have been almost retained after SFT for both the thru-view and the edge-view. Therefore the structural modification through SFT seems to be small.

To analyze the molecular orientation including the amorphous regions, a laser Raman microprobe spectroscopy is convenient. The intensity at 1615 cm^{-1}, (I_{1615}) is very sensitive to the molecular orientation of PET [8]. The authors reported previously that the intensity of I_{1615}

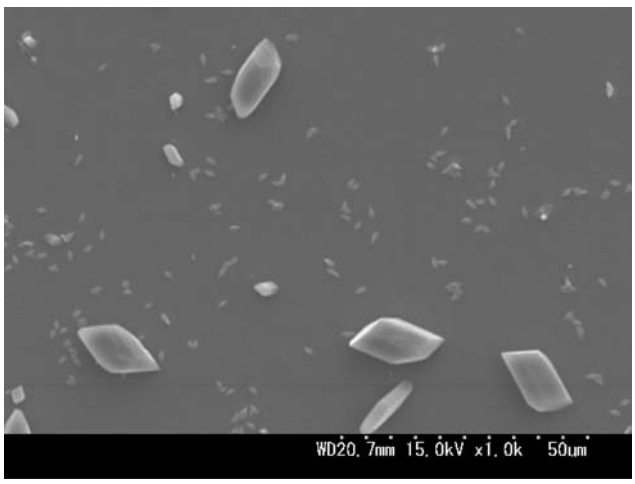

Fig. 1 SEM image for the surface of the PET film subjected to the SFT

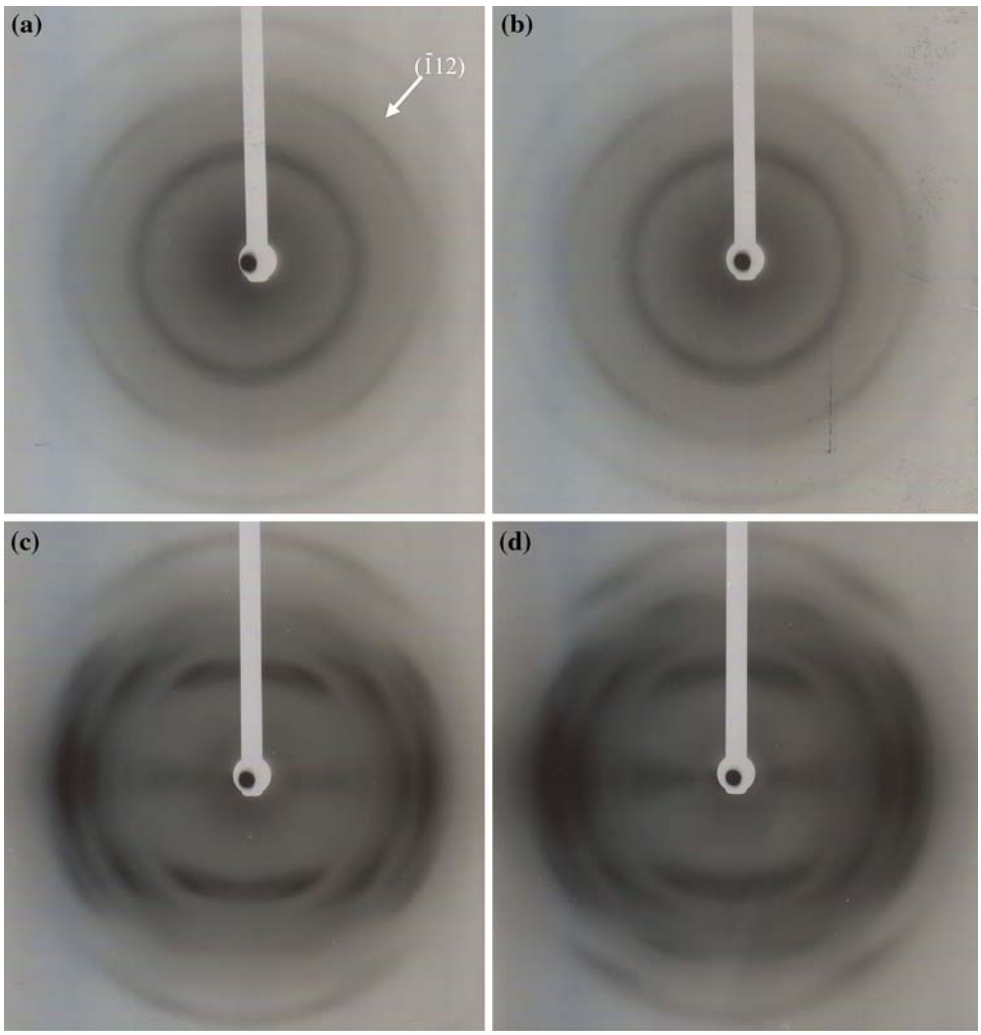

Fig. 2 WAXD patterns for the PET films. **a** and **b** are the thru-views before and after the SFT, respectively, and the vertical direction is MD and the horizontal is TD. **c** and **d** are the edge-views before and after the SFT, respectively, and the vertical direction is MD and the horizontal is thru-direction

normalized by the intensity at 632 cm^{-1} (I_{632}), i.e., I_{1615}/I_{632} is almost proportional to birefringence of PET fibers from the measurements using a laser Raman microprobe spectroscopy equipped with a polarizer [9]. Figure 3 shows Raman intensity distributions measured by rotating the polarizer from MD to TD or from MD to ThD for the PET films. It is seen that the distribution patterns have been almost unchanged. Therefore, it can be deduced that the molecular orientation for the PET films has been hardly modified through the SFT.

To investigate the change in crystalline regions, DSC measurements were made. DSC curves for the films are shown in Fig. 4. The control film only showed an endothermic peak corresponding to the fusion of crystallites, i.e., primary lamellae. The film subjected to the SFT also showed an endothermic peak in the almost same temperature range as control one. Moreover a very small and broad endothermic peak corresponding to imperfect crystallites was observed at ca. 150 °C. The data estimated from DSC measurements are summarized in Table 1. It is seen that crystallinity has slightly increased through the SFT. The peak fusion temperature for the crystallites, however, was almost unchanged. Therefore the increase in crystallinity is not due to the thickening or crystal perfecting for primary lamellae, but due to the secondary crystallization. Kong and Hay [10] investigated the multiple melting behavior of PET, and reported that the endotherm measured at ca. 150 °C is due the melting of imperfect secondary lamellae generated by the amorphous material between the primary lamellae. The endotherm measured at ca. 252 °C is predominately due to the melting of primary lamellae, but the heat for the melting of secondary lamellae generated on the surface of primary lamellae is also included in the DSC curve measured for the treated film.

As compared with the fusion peak for primary lamellae, the fusion peak for the imperfect secondary lamellae at ca. 150 °C is negligibly small. The heat of fusion for imperfect

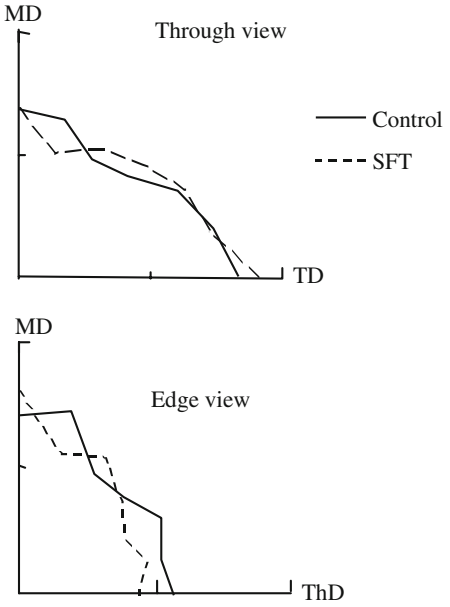

Fig. 3 Raman intensity distributions measured by rotating the polarizer from MD to TD or from MD to ThD for the PET films: solid line, control; dashed line, after the SFT

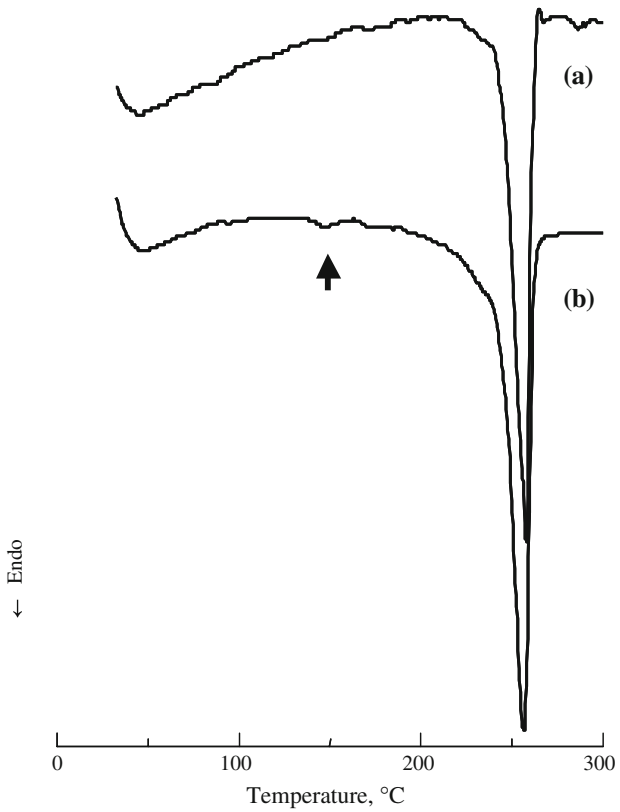

Fig. 4 DSC curves for the PET films: (a) control, (b) after the SFT

secondary lamellae estimated by DSC measurements was 0.79 J/g. The authors [4] reported previously that molecular orientation in amorphous regions is closely related to the nucleation of imperfect lamellae. In case of spin-drawing PET fibers having well-oriented amorphous chains, the heat of fusion for imperfect lamellae was 0.4 J/g. On the contrary as for the high-speed spun PET fibers having little disordered amorphous chains, the value reached to 1.4 J/g. The higher-order structures are quite different between the successive-biaxially stretched films and the one-way stretched fibers. However the degree of the orientation of amorphous chains will still influence the nucleation of imperfect lamellae. When the heat fusions for the imperfect lamellae are compared among them, the value for the films is ranked between the spin-drawing and the high-speed spun PET fibers.

Table 1 Thermal parameters estimated by DSC measurements for the PET films

Sample	Fusion of imperfect crystallite		Fusion of crystallite		Crystallinity (%)
	°C	J/g	°C	J/g	
Control	–	–	252.6	41.6	34.4
After s-CO_2	150.1	0.79	252.4	46.5	38.4

Table 2 Changes in tensile properties by s-CO_2 treatment for the PET films

Sample	Direction	Breaking load (N)	Yield load (N)	Breaking strain (%)	Tensile modulus (N)
Control	MD	13.5	8.3	80	342
	TD	14.3	8.1	76	401
After s-CO_2	MD	12.6	–	66	357
	TD	13.8	–	68	401

The tensile properties for the films are listed in Table 2. The tensile modulus has been slightly changed by the SFT. This tendency is understandable because WAXD patterns as well as Raman intensity distributions have been hardly modified through the SFT. However, the breaking loads and strains have been lowered. Figure 5 shows the tensile load versus strain curves for the films. The control films show the yield load peaks in both MD and TD. However, for the films subjected to the SFT, the yield load peaks have become ambiguous. Moreover the number of curves showing the shorter breaking strain has increased. The decrease in breaking strain means lowering of plasticity.

Strobl and co-authors [11] have analyzed the drawing process for semicrystalline polymers and have classified the process into three regimes: intralamellar slipping of crystalline blocks occurs at small deformation, whereas a stress-induced crystalline block disaggregation-recrystallization process occurs at a strain larger than the yield strain. The strain at this transition point is related to the interplay

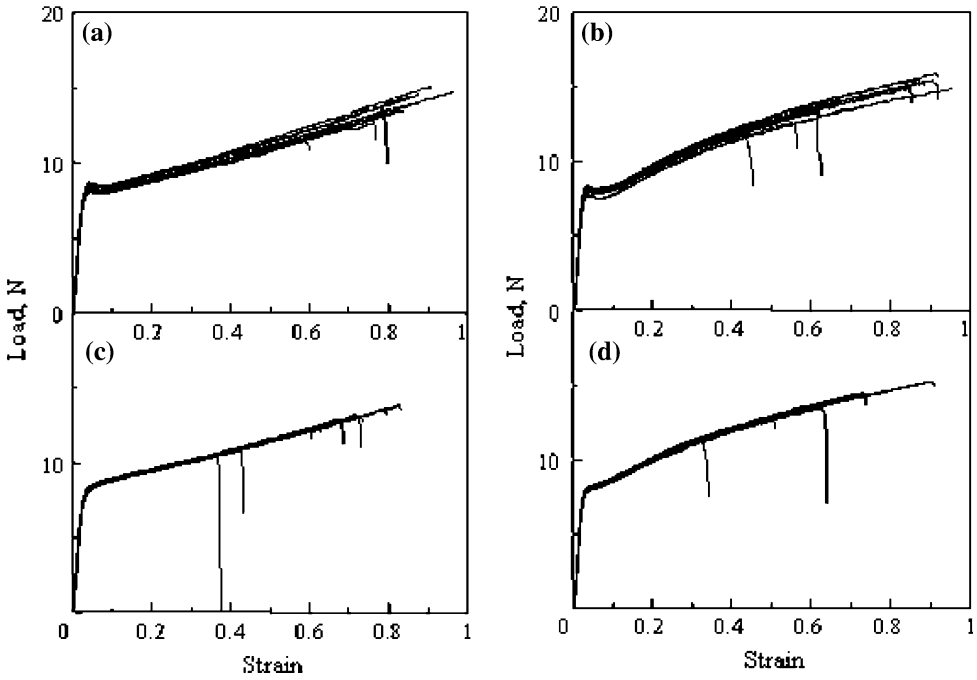

Fig. 5 Tensile load versus strain curves for the PET films. **a** and **b** are MD and TD for the control films, respectively. **c** and **d** are MD and TD for the films subjected to the SFT, respectively

between the amorphous entanglement density and the stability of crystal blocks. Tie molecules that connect adjacent lamellae are of lesser importance with respect to the deformation behavior.

The drawing of semicrystalline polymers is usually made around a temperature range a little higher than a glass transition temperature for each polymer. In the case of PET, the drawing temperature industrially used is ca. 90 °C. However, the tensile tests in this study have been made at room temperature. Thus on account of a high-glass transition temperature of PET, it is difficult to expect the intralamellar slipping of crystalline blocks or a stress-induced crystalline block disaggregation process in the tensile tests. The amorphous entanglement density or the intralamellar slipping of imperfect lamellae will become influential factors against tensile deformation.

From the tensile data in Table 2 and Fig. 5, it is seen that the tensile modulus and the yield strain are almost unchanged after the SFT. From WAXD and Raman microprobe spectroscopic analyses it is seen that the orientation of molecular chains is almost retained after the SFT. Thus it is natural to assume that the interplay between the amorphous entanglement densities will also be kept constant even though the swelling of amorphous regions with s-CO_2 occurs in the SFT. Therefore the yield strain was unchanged after the SFT. The SFT caused the secondary crystallization in two regions: (1) between the primary lamellae where imperfect secondary lamellae were generated by the amorphous material, (2) on the surface of primary lamellae. The secondary lamellae between the primary lamellae will resist deforming. However the amount of such lamellae appears to be too small to modify the tensile curve. It is probable that the increase in crystallinity caused by secondary lamellae generated and combined onto the surface of primary lamellae have brought about the decrease in amorphous chains to be deformed easily at tensile tests. Then the shape of yield peak was modified and the plasticity for the films was lowered.

Conclusions

The plasticity for the PET films was lowered when the films were subjected to the SFT. The yield load peaks became ambiguous and the breaking strains and loads decreased. DSC measurements revealed that the SFT caused the secondary crystallization in two regions: (1) between the primary lamellae where imperfect secondary lamellae were generated by the amorphous material, (2) on the surface of primary lamellae. The secondary lamellae between the primary lamellae will resist deforming. However the amount of such lamellae appears to be too small to modify the tensile curve. It is probable that the increase in crystallinity caused by secondary lamellae generated and combined onto the surface of primary lamellae have brought about the decrease in amorphous chains to be deformed easily at tensile tests.

References

1. Heffelfinger CJ, Schmidt PG (1960) J Appl Polym Sci 9:2661
2. Matsumoto K, Ieki H, Imamura R (1971) Sen'i Gakkaishi 27:516
3. Matsumoto K (1993) Film wo tsukuru. Kyoritsushuppan, Tokyo, p 99
4. Kawahara Y, Kamo M, Yamamoto K, Ogawa S, Terada D, Kikutani T, Tsuji M (2006) Macromol Mater Eng 291:11
5. Mensitieri G, Nobile MAD, Guerra G, Apicella A, Ghatta HA (1995) Polym Eng Sci 35:506
6. Roberts RC (1969) Polymer 10:113
7. Drews MJ, Jordan C (1998) Text Chem Colo 30(6):13
8. Purvis J, Bower DI (1976) J Polym Sci 14:1461
9. Terada D, Kawahara Y, Iwamoto M, Kikutani T (2002) Sen'i Gakkaishi 58:342
10. Kong Y, Hay JN (2003) Polymer 44:623
11. Men Y, Rieger J, Strobl G (2003) Phys Rev Lett 91:095502-1